Theory of Nonlinear Effects in a Gas Laser Amplifier.
I. Weak Signals*

Andrew Dienes

Bell Telephone Laboratories, Holmdel, New Jersey

(Received 19 April 1968)

Using classical fields and the density-matrix formalism, we analyze the nonlinear characteristics of a gas laser amplifier subject to an axial magnetic field, operating with two optical-frequency signals of arbitrary polarization. Perturbational solutions, valid for relatively weak intensities, are obtained which describe the saturation interaction of the signals and the generation of combination tones. An arbitrary amount of Doppler broadening is considered throughout. The simple $J=1 \rightarrow J=0$ model is found convenient to describe the physical processes taking place. In general, however, the interactions are found to depend on the J values of the levels. We find that only saturation and no combination-tone generation occurs for two opposite circularly polarized signals, while both effects are, in general, present for two linearly or elliptically polarized fields. The limiting case of zero magnetic field is examined separately. It is also found that in many cases the medium is made effectively anisotropic by the nonlinear interactions. Applications to measurements of atomic parameters such as J values, g values, and lifetimes are discussed.

1. INTRODUCTION

NONLINEAR interactions of electromagnetic fields in a population-inverted gaseous medium have received considerable attention recently. Lamb[1] has calculated saturation effects, valid for arbitrarily strong fields and stationary atoms in a single-frequency traveling-wave maser, using a scalar electromagnetic field and a model of two nondegenerate levels. Strong saturation in a gas laser amplifier was also studied by Gordon, White, and Rigden,[2] who used a rate equation approach. Lamb[3] has given the scalar theory of a multimode laser oscillator including the effects of atomic motion. The induced polarization was calculated to the third order in the fields and the results are valid for low intensities only. Aronowitz[4] has performed a single-mode calculation for a ring laser and included isotope effects.

Several attempts have been made to include the vector nature of the electromagnetic field without going to more complicated level structures. Haken and Sauermann[5] used a model of two nondegenerate levels and the "classical" method of averaging over possible atomic dipole orientations. Tang and Statz[6] used the same method with a somewhat simpler model containing one decay rate only. Close[7] has made a detailed study of a laser amplifier using Lamb's atomic model. Both

perturbational and strong-field results were obtained and the vector nature of the fields included by the method of the previous authors. The strong-field results for parallel polarized (i.e., scalar) fields were reported separately.[8]

Lamb's oscillator theory has been extended to lasers in magnetic fields, using vector fields interacting with atomic levels that are eigenstates of angular momentum. Fork and Sargent[9,10] have given amplitude and frequency-determining equations for axial magnetic field and a $J=1 \rightarrow J=0$ transition. Culshaw and Kannelaud have treated the $J=\frac{1}{2} \rightarrow J=\frac{1}{2}$ transition in axial field[11] and the $J=1 \rightarrow J=0$ transition in axial as well as transverse magnetic field.[12] Durand[13,14] also treated the $J=1 \rightarrow J=0$ laser using a rate equation approach. D'Yakonov and Perel[15] gave a theory for an arbitrary $J_a \rightarrow J_b$ transition valid for weak axial magnetic field. Heer and Graft[16] outlined a very general theory valid for amplifiers, standing wave or ring lasers. They included atoms with arbitrary angular momenta and hyperfine structure, magnetic field at arbitrary angle to the direction of propagation. However, they did not evaluate the coefficients in their expressions. In zero magnetic field calculations of a $J_a \rightarrow J_b$ transition Polder and Van Haeringen[17] and Doyle and White[18] obtained results for the polarization

[1] W. E. Lamb, Jr., in *Lectures in Theoretical Physics*, edited by W. E. Brittin and B. W. Downs (Interscience Publishers, Inc., New York, 1960).
[2] E. I. Gordon, A. D. White, and J. D. Rigden, in *Proceedings of the Symposium on Optical Masers at the Polytechnic Institute of Brooklyn, April, 1963* (Polytechnic Press, Brooklyn, New York, 1963).
[3] W. E. Lamb, Jr., Phys. Rev. 134, A1429 (1964).
[4] F. Aronowitz, Phys. Rev. 139, A635 (1965).
[5] H. Haken and H. Sauermann, Z. Physik 176, 47 (1963).
[6] C. L. Tang and H. Statz, Phys. Rev. 128, 1013 (1962).
[7] D. H. Close, Scientific Report No. 5 AF 49 (638)-1322, 1965 (unpublished); Ph.D. thesis, California Institute of Technology, 1965 (unpublished).

[8] D. H. Close, Phys. Rev. 153, 360 (1967).
[9] R. L. Fork and M. Sargent, III, Phys. Rev. 139, A617 (1965).
[10] R. L. Fork and M. Sargent, III, in *Proceedings of the Physics of Quantum Electronics Conference, San Juan, Puerto Rico, 1965*, edited by P. L. Kelley, B. Lax, and P. E. Tannenwald (McGraw-Hill Book Co., New York, 1965).
[11] W. Culshaw and J. Kannelaud, Phys. Rev. 141, 228 (1966).
[12] W. Culshaw and J. Kannelaud, Phys. Rev. 145, 258 (1966); 156, 308 (1967).
[13] G. Durand, Ann. Inst. Henri Poincaré A4, 263 (1966).
[14] G. Durand, IEEE J. Quantum Electron. QE-2, 448 (1966).
[15] M. I. D'Yakonov and V. E. Perel, Opt. i Spektroskopiya 20, 472 (1966) [English transl.: Opt. Spectry. (USSR) 20, 257 (1966)].
[16] C. V. Heer and R. D. Graft, Phys. Rev. 140, A1088 (1965).
[17] D. Polder and W. Van Haeringen, Phys. Letters 19, 380 (1965); W. Van Haeringen, Phys. Rev. 158, 256 (1967).
[18] W. M. Doyle and M. B. White, Phys. Rev. 147, 359 (1966); Phys. Rev. Letters 17, 467 (1966).

states of the modes in a laser oscillator. More recently Sargent, Lamb, and Fork[19] gave a detailed theory of a Zeeman laser oscillator with numerical results covering a general state of polarization in the cavity, any degree of cavity anisotropy, arbitrary angular momenta, and hyperfine structure. As in Lamb's scalar theory[3] and in Refs. 9–19, the induced polarization is calculated to third order in a perturbational series giving results valid for weak fields. Some results on combination-tone generation in a magnetically tuned laser amplifier were reported by this author.[20] In this paper we give a theory of nonlinear interactions of electromagnetic waves of arbitrary polarization in a laser amplifier subject to an axial magnetic field. The zero magnetic field case is also considered. In addition to the perturbational results, we also obtained equations that are valid for arbitrarily strong field intensities. These are presented in II.[21] The velocity integrals are evaluated exactly throughout and the results are consequently valid for any amount of Doppler broadening. (This is especially important for the strong-field results of II, since at high intensities even a strongly inhomogeneous line becomes partly homogeneous.) There is, so to speak, one more degree of freedom in a laser amplifier than in an oscillator. The frequencies and polarization states of the fields are not determined by the cavity and the active medium. They can be entirely arbitrary. This generality is fully explored in this paper. Emphasis is placed on the interpretation of the results in terms of the physical processes that take place. Both a simple $J=1 \rightarrow J=0$ and a general $J_a \rightarrow J_b$ transition are considered. Collision effects are ignored.

We are concerned principally with two nonlinear effects which we call saturation interaction and combination-tone generation. Before proceeding to calculate them it is useful to discuss briefly the nature of these effects. Figure 1 shows schematically a simple $J=1 \rightarrow J=0$ level system where the sublevels are split by an applied magnetic field. The polarization vector of the dipole moment is indicated for each transition. Gain nonlinearities are caused by self-saturation of the circularly polarized components, by cross saturation due to transitions terminating on a common level, and by double quantum interactions in which an atom
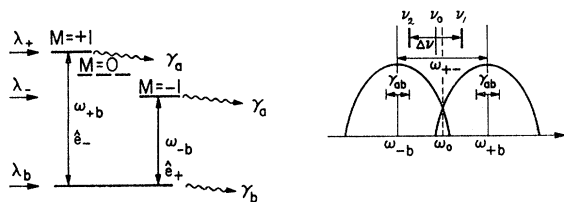
acquires an electric quadrupole by interacting coherently with a left and a right circular field. These physical processes occur regardless of the polarization states of the input fields, and are exhibited in the calculations that follow.

If the electromagnetic field $E(z, t)$ contains two frequencies ν_1 and ν_2, new frequencies can appear in the laser due to nonlinearities of the medium. $[E(z, t)]^3$ can contain terms oscillating at $2\nu_2-\nu_1$ and $2\nu_1-\nu_2$, $[E(z, t)]^5$ terms at $3\nu_2-2\nu_1$ and $3\nu_1-2\nu_2$ in addition, etc.[22] This effect we may call combination-tone generation. Physically it is caused by a coherent modulation of the population-inversion densities. If a given transition is acted on by two fields of frequencies ν_1 and ν_2, an atom in either state of that transition sees a field with beats at frequency $\Delta\nu=\nu_1-\nu_2$, and the population inversion is modulated. Because the gain is proportional to the population inversion, this results in a parametric generation of new frequencies at $\nu_1 \pm n\Delta\nu$. The necessary condition for this process is that two (or more) fields of different frequency must be connecting the two levels of a given transition. If different transitions are involved no combination-tone generation occurs unless the relevant sublevels are connected by some other interaction such as collisions. We expect therefore that no combination tones occur in our laser amplifier for two opposite circularly polarized input signals, but that combination tones can be observed for two linearly or elliptically polarized waves.

2. ELECTROMAGNETIC FIELD AND THE POLARIZATION OF THE MEDIUM

In order to keep our results both tractable and sufficiently general, we shall assume that the electromagnetic field consists of two nearly monochromatic plane waves of frequencies ν_1 and ν_2, with arbitrary polarization states, propagating in the z direction. It will be found convenient, however, to work with circularly polarized waves. Accordingly, the field at each frequency will consist of two opposite circularly polarized components. Defining a vector base system by

$$\mathbf{E} = \sum_{m=0,\pm} \hat{e}_m E_m, \qquad (1)$$

where $\hat{e}_\pm = (1/\sqrt{2})(\hat{e}_x \pm i\hat{e}_y)$ and $\hat{e}_0 = \hat{e}_z$ and $E_m = \mathbf{E} \cdot \hat{e}_m^*$, the electromagnetic field is

$$\mathbf{E}(t, z) = \mathrm{Re}\{\hat{e}_+ E_{1+} \exp i(k_1 z - \nu_1 t + \phi_{1+})$$

$$+\hat{e}_- E_{1-} \exp i(k_1 z - \nu_1 t + \phi_{1-}) + \hat{e}_+ E_{2+} \exp i(k_2 z - \nu_2 t + \phi_{2+})$$

$$+\hat{e}_- E_{2-} \exp i(k_2 z - \nu_2 t + \phi_{2-})\}. \quad (2)$$

E_{jm} and ϕ_{jm} are slowly varying functions of position and time. Arbitrary linear, circular, and elliptical waves result by choosing the magnitudes and initial phases appropriately. For convenience, k is taken to be equal to the free-space propagation constant ν_i/c, and the

FIG. 1. The $J=1$ to $J=0$ transition.

[19] M. Sargent, III, W. E. Lamb, Jr., and R. L. Fork, Phys. Rev. 164, 436 (1967); 164, 450 (1967).
[20] A. Dienes, Appl. Phys. Letters 9, 142 (1966).
[21] A. Dienes, following paper, Phys. Rev. 174, 414 (1968), hereafter referred to as II.

[22] E. O. Schulz-Du Bois, Proc. IEEE 52, 644 (1964).

total phase shift due to the medium is accounted for by ϕ_{jm}.

The polarization of the medium is obtained by calculating the expectation value of the dipole moment for a single atom and summing up over all atoms that at some time are excited to the pertinent energy levels. The method used for the perturbational calculations is similar to that of Sargent, Lamb, and Fork,[19] and only its outlines will be given. The equation of motion for the truncated atomic density matrix ρ is[23]

$$i\dot{\rho} = [H_0 - \tfrac{1}{2}(i\hbar\Gamma)]\rho - \rho[H_0 + \tfrac{1}{2}(i\hbar\Gamma)] + H'\rho - \rho H', \quad (3)$$

where H_0 is the unperturbed Hamiltonian, $H' = -\mathbf{p}\cdot\mathbf{E}$ is the interaction Hamiltonian, and Γ is the phenomenological decay constant matrix. The macroscopic density matrix $\rho(z, v, t, \hat{t})$ is defined by

$$\rho(z, v, t, \hat{t}) = \sum_\alpha \int_{-\infty}^{t} dt_0 \int dr_0 \, \lambda_\alpha(z_0, t_0, v)$$
$$\times \rho(\alpha, z_0, t_0, v, \hat{t}) \delta[z - z_0 - v(t - t_0)]. \quad (4)$$

$\rho(\alpha, z_0, t_0, v, \hat{t})$ is the density matrix, at time $\hat{t}$, of an atom that is excited to the level α at time t_0 and position z_0 with velocity v, and $\lambda_\alpha(z_0, t_0, v)$ is the density of excitation per unit time per unit volume. Thus $\rho(z, v, t, \hat{t})$ describes an ensemble of atoms at time $\hat{t}$. These atoms are moving with velocity v and at time t are located at the position z. The equation of motion of the macroscopic density matrix is

$$id\rho(z, v, t, \hat{t})/dt = [H_0 - \tfrac{1}{2}(i\hbar\Gamma)]\rho - \rho[H_0 + \tfrac{1}{2}(i\hbar\Gamma)]$$
$$+ H'\rho - \rho H' + i\lambda_\alpha(z, v, t). \quad (5)$$

The induced polarization due to atoms of velocity v is

$$\mathbf{P}(z, t, v) = \text{Tr}[\mathbf{p}\rho(z, v, t, t)]. \quad (6)$$

The total macroscopic polarization is found by integrating over all velocities. In this paper the set of equations implied by (5) are solved by iteration, and $\mathbf{P}$ is calculated to third order in the fields. First, the simple $J=1 \rightarrow J=0$ transition is treated in some detail. Next, the results are extended to the general $J_a \rightarrow J_b$ transition.

3. $J=1$ TO $J=0$ TRANSITION

The energy diagram, showing the interaction with the electromagnetic field, the spontaneous decay rates, and the pumping of the levels, is given in Fig. 1. Defining

$$P_{jm}(z, t, v) = \text{Re}[\mathcal{P}_{jm}(v) \, \exp i(k_j z - \nu_j t + \phi_{jm})], \quad (7)$$

and

$$\mathcal{L}_+(\omega, \nu) = \gamma_{ab}[\gamma_{ab} + i(\omega - \nu + kv)]^{-1}, \quad (8a)$$

$$\mathcal{L}_-(\omega, \nu) = \gamma_{ab}[\gamma_{ab} - i(\omega - \nu + kv)]^{-1}, \quad (8b)$$

we find the left circular component of the polarization at the input frequency ν_1 to be

$$(\nu/2\epsilon_0 c)\mathcal{P}_{1-}(v) = -i\alpha W(v) E_{1-}\mathcal{L}_+(\omega_{+b}, \nu_1)\{1 - (E_{1-}^2/2E_0^2)[\mathcal{L}_+(\omega_{+b}, \nu_1) + \mathcal{L}_-(\omega_{+b}, \nu_1)]$$

$$- (E_{2-}^2/2E_0^2)[\mathcal{L}_+(\omega_{+b}, \nu_2) + \mathcal{L}_-(\omega_{+b}, \nu_2)] - (E_{2-}^2/2E_0^2)(\gamma_a\gamma_b/2\gamma_{ab})[(\gamma_a - i\Delta\nu)^{-1} + (\gamma_b - i\Delta\nu)^{-1}]$$

$$\times [\mathcal{L}_+(\omega_{+b}, \nu_1) + \mathcal{L}_-(\omega_{+b}, \nu_2)] - (E_{1+}^2/2E_0^2)(\gamma_a/2\gamma_{ab})[\mathcal{L}_+(\omega_{-b}, \nu_1) + \mathcal{L}_-(\omega_{-b}, \nu_1)]$$

$$- (E_{2+}^2/2E_0^2)(\gamma_a/2\gamma_{ab})[\mathcal{L}_+(\omega_{-b}, \nu_2) + \mathcal{L}_-(\omega_{-b}, \nu_2)] - (E_{1+}^2/2E_0^2)(\gamma_a\gamma_b/2\gamma_{ab})$$

$$\times (\gamma_a + i\omega_{+\,-})^{-1}[\mathcal{L}_+(\omega_{+b}, \nu_1) + \mathcal{L}_-(\omega_{-b}, \nu_1)] - (E_{2+}^2/2E_0^2)(\gamma_a\gamma_b/2\gamma_{ab})[\gamma_a + i(\omega_{+\,-} - \Delta\nu)]^{-1}$$

$$\times [\mathcal{L}_+(\omega_{+b}, \nu_2) + \mathcal{L}_-(\omega_{-b}, \nu_2)]\} + i\alpha W(v)(E_{1+}E_{2+}E_{2-}/2E_0^2)(\gamma_a\gamma_b/2\gamma_{ab})\{(\gamma_b - i\Delta\nu)^{-1}$$

$$\times [\mathcal{L}_+(\omega_{-b}, \nu_1) + \mathcal{L}_-(\omega_{-b}, \nu_2)]\mathcal{L}_+(\omega_{+b}, \nu_2) + (\gamma_a + i\omega_{+\,-})^{-1}[\mathcal{L}_+(\omega_{+b}, \nu_2) + \mathcal{L}_-(\omega_{-b}, \nu_2)]\mathcal{L}_+(\omega_{+b}, \nu_1)\}\exp(i2\theta). \quad (9)$$

The constant $\alpha_0 = N_0\nu |\langle a \| p \| b \rangle|^2/6\epsilon_0\hbar c\gamma_{ab}$ is the small-signal gain parameter, where $N_0 = \lambda_a/\gamma_a - \lambda_b/\gamma_b$ is the excitation density and $\langle a \| p \| b \rangle$ is the reduced matrix element of the dipole operator $\mathbf{p}$. E_0^2 is the saturation field intensity, defined by

$$E_0^2 = 3\hbar^2\gamma_a\gamma_b/|\langle a \| p \| b \rangle|^2,$$

and $W(v)$ is the velocity distribution, assumed to be Maxwellian, with average velocity v.

$$\theta = \Phi_2 - \Phi_1 = \tfrac{1}{2}[(\phi_{2-} - \phi_{2+}) - (\phi_{1-} - \phi_{1+})]$$

is the angle between the major axes. The $\omega_{\pm b}$ are the atomic transition frequencies originating on the $M = \pm 1$ sublevels, respectively, and $\omega_{+\,-} = \omega_{+b} - \omega_{-b}$ is the Zeeman separation of the two circularly polarized transitions. The right circular component $(\nu/2\epsilon_0 c)\mathcal{P}_{1+}(v)$ is obtained from Eq. (10) by interchanging $+$ and $-$ subscripts. Similar expressions hold for $(\nu/2\epsilon_0 c)\mathcal{P}_{2\pm}$ which we get from the above by interchanging subscripts 1 and 2.

In addition, this third-order calculation gives two new frequency components, or combination tones, at the frequencies $\nu_0 = 2\nu_1 - \nu_2$ and $\nu_3 = 2\nu_2 - \nu_1$. These are

$$(\nu/2\epsilon_0 c)\mathcal{P}_{0-}(\nu) = i\alpha W(\nu)\mathcal{L}_+(\omega_{+b}, 2\nu_1 - \nu_2)\{(E_{1-}^2 E_{2-}/2E_0^2)(\gamma_a\gamma_b/2\gamma_{ab})[(\gamma_a - i\Delta\nu)^{-1} + (\gamma^b - i\Delta\nu)^{-1}]$$

$$\times [\mathcal{L}_+(\omega_{+b}, \nu_1) + \mathcal{L}_-(\omega_{+b}, \nu_2)] + (E_{1-}E_{1+}E_{2+}/2E_0^2)(\gamma_a\gamma_b/2\gamma_{ab})[(\gamma_b - i\Delta\nu)^{-1}\mathcal{L}_+(\omega_{-b}, \nu_1) + \mathcal{L}_-(\omega_{-b}, \nu_2)]$$

$$+ [\gamma_a + i(\omega_{+-} - \Delta\nu)]^{-1}[\mathcal{L}_+(\omega_{+b}, \nu_1) + \mathcal{L}_-(\omega_{-b}, \nu_2)]\}\exp i[2\theta]\}, \quad (10)$$

[23] L. R. Wilcox and W. E. Lamb, Jr., Phys. Rev. **119**, 1915 (1960).

and similar expressions for the other three components. The total polarization is calculated by performing the integration over the velocity distribution. The integrals are expressed in terms of the error function of complex argument,[24] defined by

$$w(z) = \exp(-z^2)\ \mathrm{erfc}(-iz) = (2/\sqrt{\pi})\ \exp(-z^2) \int_z^\infty \exp(-t^2)\,dt. \tag{11}$$

This is related to the "plasma dispersion function" by

$$w(x+iy) = -i\pi^{-1/2}Z(x+iy). \tag{12}$$

The result is

$$(\nu/2\epsilon_0 c)\mathcal{P}_{1-} = -i\alpha E_{1-}\{w^*(x_0+y-\eta+ia) - (E_{1-}^2/2E_0^2)H_1(x_0, y, \eta) - (E_{1+}^2/2E_0^2)[H_2(x_0, y, \eta) + H_3(x_0, y, \eta)]$$

$$- (E_{2-}^2/2E_0^2)[H_4(x_0, y, \eta) + H_5(x_0, y, \eta)] - (E_{2+}^2/2E_0^2)[H_6(x_0, y, \eta) + H_7(x_0, y, \eta)]\}$$

$$+ i\alpha(E_{1+}E_2\_E_{2+}/2E_0^2)[H_8(x_0, y, \eta) + H_9(x_0, y, \eta)], \tag{13}$$

where

$$H_1 = a\{2/\sqrt{\pi} - 2[a+i(x_0+y-\eta)]w^*(x_0+y-\eta+ia) + (1/a)\,\mathrm{Re}\,w^*(x_0+y-\eta+ia)\}, \tag{14}$$

$$H_2 = A(i/2y)[w^*(x_0+y-\eta+ia) - w^*(x_0-y-\eta+ia)] + [0.5/(a+iy)][w^*(x_0+y-\eta+ia) + w(x_0-y-\eta+ia)], \tag{15}$$

$$H_3 = [AB/(A+iy)]\{2/\sqrt{\pi} - 2[a+i(x_0+y-\eta)] \times w^*(x_0+y-\eta+ia) + [0.5/(a+iy)] \times [w^*(x_0+y-\eta+ia) + w(x_0-y-\eta+ia)]\}, \tag{16}$$

$$H_4 = a\{(i/2\eta)[w^*(x_0+y+\eta+ia) - w^*(x_0+y-\eta+ia)] + [0.5/(a-i\eta)][w^*(x_0+y-\eta+ia) + w(x_0+y+\eta+ia)]\}, \tag{17}$$

$$H_5 = AB[(A-i\eta)^{-1} + (B-i\eta)^{-1}] \times \{2/\sqrt{\pi} - 2[a+i(x_0+y-\eta)]w^*(x_0+y-\eta+ia) + [0.5/(a-i\eta)][w^*(x_0+y-\eta+ia) + w(x_0+y+\eta+ia)]\}, \tag{18}$$

$$H_6 = A\{[i/2(y-\eta)][w^*(x_0+y-\eta+ia) - w^*(x_0-y+\eta+ia)] + 0.5[a+i(y-\eta)]^{-1} \times [w^*(x_0+y-\eta+ia) + w(x_0-y+\eta+ia)]\}, \tag{19}$$

$$H_7 = AB[A+i(y-\eta)]^{-1}\{2/\sqrt{\pi} - 2[a+i(x_0+y-\eta)] \times w^*(x_0+y-\eta+ia) + 0.5[a+i(y-\eta)]^{-1} \times [w^*(x_0+y-\eta+ia) + w(x_0-y+\eta+ia)]\}, \tag{20}$$

$$H_8 = [AB/(B-i\eta)]\{(i/2y)[w^*(x_0+y-\eta+ia) - w^*(x_0-y-\eta+ia)] + 0.5[a+i(y-\eta)]^{-1} \times [w^*(x_0+y+\eta+ia) + w(x_0-y+\eta+ia)]\}\exp[i2\theta], \tag{21}$$

$$H_9 = [AB/(A+iy)]\{(i/2\eta)[w^*(x_0+y+\eta+ia) - w^*(x_0+y-\eta+ia)] + 0.5[a+i(y-\eta)]^{-1} \times [w^*(x_0+y-\eta+ia) + w(x_0-y+\eta+ia)]\}\exp[i2\theta] \tag{22}$$

with the limiting case

$$\lim_{\Delta\to 0} (0.5i/\Delta)[w^*(z+\Delta+ia) - w^*(z-\Delta+ia)]$$

$$= 2/\sqrt{\pi} - 2(a+iz)w^*(z+ia). \tag{23}$$

In the above equations,

$x_0 = [(\omega_{+b}+\omega_{-b}) - (\nu_1+\nu_2)]/2ku = (\omega_0-\nu_0)/ku$, the detuning of the mean frequency from line center;

$y = (\omega_{+b}-\omega_{-b})/2ku = \omega_{+\ -}/2ku$, the Zeeman shift or half the line separation;

$\eta = (\nu_1-\nu_2)/2ku = \Delta\nu/2ku$, half the frequency separation of the input signals;

$a = \gamma_{ab}/ku$, the natural linewidth;

$A = \gamma_a/2ku$, $B = \gamma_b/2ku$, the decay rates of the upper and lower levels.

All the above are given in units of the Doppler width parameter ku. The quantity

$$\alpha = a\alpha_0 = N_0\sqrt{\pi}\nu\,|\langle a\,||\,p\,||\,b\rangle|^2/6\epsilon_0\hbar cku$$

is the small-signal inhomogeneous gain constant.

To obtain the other three components of the polarization the following simple rules are to be used:

$\mathcal{P}_{1m}\to\mathcal{P}_{2m}$ interchange subscripts 1 and 2, let $\eta\to-\eta$;

$\mathcal{P}_{j-}\to\mathcal{P}_{j+}$ interchange subscripts $+$ and $-$, let $y\to -y$.

The new frequency, or combination-tone, components are calculated from (10) in the same manner.

$$(\nu/2\epsilon_0 c)P_{0-} = i\alpha\{(E_{1-}^2E_2\_/2E_0^2)U_1(x_0, y, \eta) + (E_{1-}E_{1+}E_{2+}/2E_0^2)[U_2(x_0, y, \eta) + U_3(x_0, y, \eta)]\}$$

$$\times\exp[i2\theta], \tag{24}$$

[24] Handbook of Mathematical Functions, edited by M. Abramowitz and I. A. Stegun (National Bureau of Standards, Washington, D. C., 1964), Appl. Math. Series, Vol. 55, pp. 297–304, 325–328.
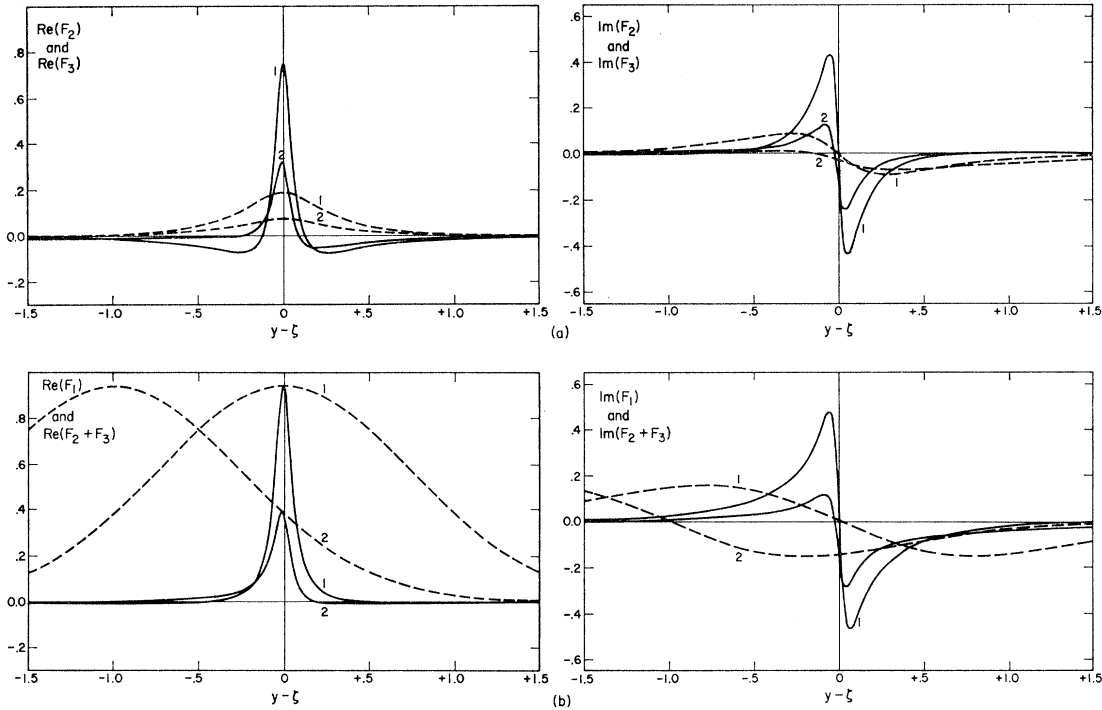
FIG. 2. The nonlinear polarization functions: $A = 0.06$, $B = 0.24$, $a = 0.3$; (a) H_2 (dash) and H_3 (solid); (b) H_1 (dash) and $H_2 + H_3$ (solid); (1) $x_0 = 0$; (2) $x_0 = 1.0$. Note that F is used in place of H in the axis labels.

where

$$U_1 = AB[(A - i\eta)^{-1} + (B - i\eta)^{-1}]$$

$$\times \{ (i/2\eta)[w^*(x_0 + y - \eta + ia) - w^*(x_0 + y - 3\eta + ia)]$$

$$+ [0.5/(a - 2\eta)][w^*(x_0 + y - 3\eta + ia)$$

$$+ w(x_0 + y + \eta + ia)]\}, \quad (25)$$

$$U_2 = [AB/(B - i\eta)]\{[i/2(y - \eta)][w^*(x_0 + y - 3\eta + ia)$$

$$- w^*(x_0 - y - \eta + ia)] + \tfrac{1}{2}[a + i(y - 2\eta)]^{-1}$$

$$\times [w^*(x_0 + y - 3\eta + ia) + w(x_0 - y + \eta + ia)]\}, \quad (26)$$

$$U_3 = AB[A + i(y - \eta)]^{-1}\{ (i/2\eta)[w^*(x_0 + y - \eta + ia)$$

$$- w^*(x_0 + y - 3\eta + ia)] + \tfrac{1}{2}[a + i(y - 2\eta)]^{-1}$$

$$\times [w^*(x_0 + y - 3\eta + ia) + w(x_0 - y + \eta + ia)]\}. \quad (27)$$

The rules for obtaining $\mathcal{P}_{0+}$, $\mathcal{P}_{3+}$, and $\mathcal{P}_{3-}$ are

$\mathcal{P}_{0m} \rightarrow \mathcal{P}_{3m}$ interchange subscripts 1 and 2, let $\eta \rightarrow -\eta$;

$\mathcal{P}_{j+} \rightarrow \mathcal{P}_{j-}$ interchange subscripts $+$ and $-$, let $y \rightarrow -y$.

Each of the functions $H_1 - H_9$ and $U_1 - U_3$ consists of two parts. It can be shown[7,25] that for strongly inhomogeneous broadening $(a = \gamma_{ab}/ku \rightarrow 0)$ the first part in each is negligibly small, while for homogeneous broadening $(a \rightarrow \infty)$ both parts contribute equally and

[25] H. R. Schlossberg and A. Javan, Phys. Rev. 150, 267 (1966).

the nonlinear interactions are twice as strong as in the previous case.

A. Two Opposite Circularly Polarized Signals

For this case, only E_{1-} and E_{2+} are present. $P_{0\pm}$ and $P_{3\pm}$, the new frequency terms of the induced polarization, are identically zero. This agrees with our qualitative prediction that there are no combination tones for opposite circularly polarized fields. P_{1-} and P_{2+}, the polarization terms at the input frequencies, consist only of the linear term and those nonlinear terms involving H_1, H_6, and H_7. P_{1+} and P_{2-} vanish identically, indicating that left circular wave does not generate right circular and vice versa. Substituting $\mathbf{E}$ and $\mathbf{P}$ into Maxwell's equations, neglecting transverse derivatives and such higher-order derivatives as $\partial^2 E/\partial z^2$, $\partial^2 \phi/\partial z^2$, $(\partial \phi/\partial z)(\partial E/\partial z)$, etc., we obtain the two equations

$$[\partial \phi_{jm}/\partial z + c^{-1}(\partial \phi_{jm}/\partial t)]E_{jm} = (\nu/2\epsilon_0 c)\mathcal{P}_{jmc}, \quad (28a)$$

$$\partial E_{jm}/\partial z + c^{-1}(\partial E_{jm}/\partial t) = (\nu/2\epsilon_0 c)\mathcal{P}_{jms}, \quad (28b)$$

where $\mathcal{P}_{jm} = \mathcal{P}_{jmc} - i\mathcal{P}_{jms}$ and only the subscripts $1-$ and $2+$ are allowed. Assuming that the spectral width of the field components is much smaller than their frequency separation, the field amplitudes can be chosen as purely space or purely time-dependent. The former is appropriate for the treatment of an amplifier while the latter is suitable for a ring laser. Setting time derivatives equal to zero we obtain the amplifier gain and
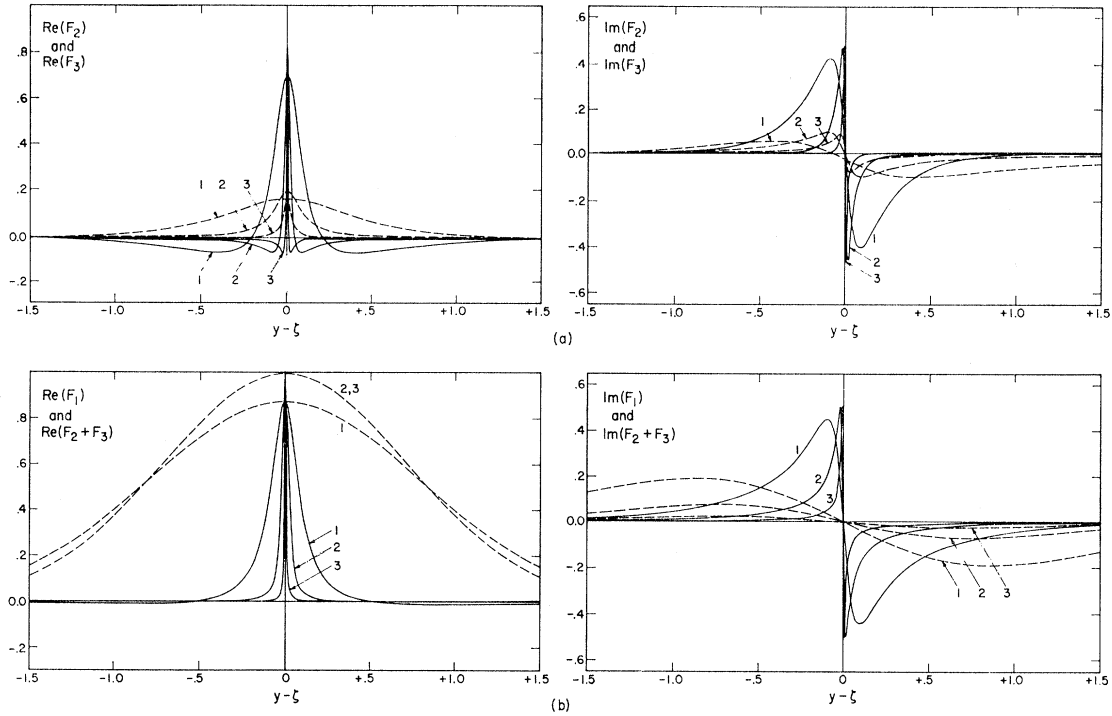
FIG. 3. The nonlinear polarization functions: $x_0=0$; (a) H_2 (dash) and H_3 (solid); (b) H_1 (dash) and H_2+H_3 (solid); (1) $a=0.5$, $A=0.1$, $B=0.4$; (2) $a=0.1$, $A=0.02$, $B=0.08$; (3) $a=0.03$, $A=0.005$, $B=0.025$. Note that F is used in place of H in the axis labels.

phase equations (1 and 2 are suppressed in the subscripts):

$$dE_-/dz = \alpha_- E_- - \beta_- E_-^3 - \theta_{-+} E_- E_+^2, \quad (29a)$$

$$dE_+/dz = \alpha_+ E_+ - \beta_+ E_+^3 - \theta_{+-} E_+ E_-^2, \quad (29b)$$

$$d\phi_-/dz = \sigma_- + \rho_- E_-^2 + \tau_{-+} E_+^2, \quad (29c)$$

$$d\phi_+/dz = \sigma_+ + \rho_+ E_+^2 + \tau_{+-} E_-^2, \quad (29d)$$

where

$$\alpha_- = \alpha\,\mathrm{Re}w^*(x_0+y-\eta+ia), \quad (30a)$$

$$\beta_- = (\alpha/2E_0^2)\,\mathrm{Re}H_1(x_0, y, \eta), \quad (30b)$$

$$\theta_{-+} = (\alpha/2E_0^2)\,\mathrm{Re}[H_6(x_0, y, \eta)+H_7(x_0, y, \eta)], \quad (30c)$$

$$\sigma_- = \alpha\,\mathrm{Im}w(x_0+y-\eta+ia), \quad (30d)$$

$$\rho_- = (\alpha/2E_0^2)\,\mathrm{Im}H_1(x_0, y, \eta), \quad (30e)$$

$$\tau_{-+} = (\alpha/2E_0^2)\,\mathrm{Im}[H_6(x_0, y, \eta)+H_7(x_0, y, \eta)]. \quad (30f)$$

The corresponding quantities with subscripts $-$ and $+$ reversed are given by letting y, $\eta \rightarrow -y$, $-\eta$.

These equations are analogous to those of Lamb[3] and other authors[9–12,18,19] for laser oscillators. For the amplifier, space derivatives replace time derivatives and incremental phase shifts are used in place of frequency shifts. In addition, there is no equivalent of the cavity losses for our case. It is instructive to examine the characteristics of the three functions H_1, H_6, and H_7. Each describes a different nonlinear effect. Their behavior is shown graphically in Figs. 2 and 3.

The function H_1 describes the self-saturation, or the nonlinear interaction of the field components with themselves. This effect is independent of the relative sizes of the decay rates γ_a and γ_b, and its variation with any one of the frequency variables is the same. Just as the linear gain function, the real part of H_1 is maximum at $x_0 \pm y \mp \eta = (\omega_{\mp b} - \nu_\pm)/ku = 0$ (when the signal is tuned to the center of the corresponding transition) and the width is approximately equal to the Doppler width. These properties are consistent with the physical description of self-saturation: The signals deplete the upper and fill up the lower level populations of the transitions, and thus burn holes in the population inversions. In addition, it is seen from Fig. 2 that while the real part is quite insensitive to variations of a (in fact increasing somewhat with decreasing a) the imaginary part decreases with a and is negligible for $a=0.03$. This property can be explained by the fact that for an inhomogeneously broadened line it is the atoms Doppler shifted away from resonance that contribute primarily to the phase shift, while those on or near resonance determine the gain. Thus the atoms responsible for the gain and therefore subject to saturation do not influence the phase shift. However, for a homogeneous line where the same atoms cause the gain and the phase shift, the third-order correction to each of these quantities is equally important. The sum H_6+H_7 is the total interaction between the two opposite circularly polarized waves. H_6 is a saturation term, due to the common lower level of the two transitions. The $+$ field, for
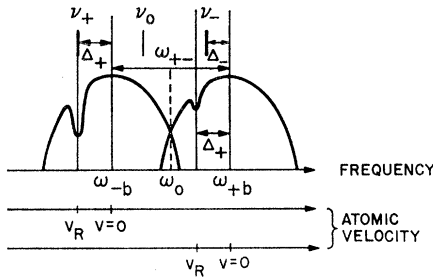
Fig. 4. Hole-burning interpretation of the behavior of F_2.

example, depletes the population inversion of the $-$ field by filling up the common lower level. By its nature, this coupling must be weaker than the self-saturation since the upper level is not influenced and the effect of one field on the population inversion of the other is therefore smaller than that on its own. The strength of this interaction (both real and imaginary parts) depends on the relative sizes of γ_a, γ_b. If $\gamma_a \ll \gamma_b$ the common level decays much quicker than the other one and H_6 is negligibly small. Equation (19) also shows that this part of the nonlinear polarization has a resonance at $y - \eta = 0$, where the signal frequency separation equals the Zeeman splitting, with a width equal to $2a = 2\gamma_{ab}/ku$. However, when we vary the detuning x_0 about zero while keeping $y - \eta$ fixed, the interaction has width 2 about $x_0 = 0$. These properties can be explained physically in terms of hole burning.[26] Each signal burns a hole not only in its own Doppler gain profile, but also in that of the other signal. This situation is shown in Fig. 4. For the sake of graphical simplicity only the holes made by the right circular (ν_+) signal are shown. The atoms involved are those traveling with velocity v_R, such that $\nu_-(1-v_R/c) = \omega_{+b}$. Because the width of the holes equals the natural linewidth $2\gamma_{ab}$, only when $|\Delta_- - \Delta_+| < 2\gamma_{ab}$ is there significant saturation interaction between the left and right circular waves. The above condition can be written as $|(\omega_{+b} - \nu_-) - (\omega_{-b} - \nu_+)| = |\omega_{+-} - \Delta\nu| < 2\gamma_{ab}$, which leads to the behavior discussed above. Variation of $\omega_0 - \nu_0$ (i.e., x_0), on the other hand, merely introduces a slowly varying Doppler weighting function.

The cross saturation described by H_7 is due to a coherent interaction of an atom with both fields. This results in a coherence of the magnetic sublevels, manifested by a nonzero ρ_{+-}. The relative magnitude of this interaction compliments that of the common level interaction: H_7 is large when $\gamma_a \ll \gamma_b$ and vice versa. This double quantum process has the characteristics of the Raman effect. That is, it remains significant only if the frequency separation $\Delta\nu \sim \omega_{+-}$. The width depends only on γ_a, the width of the upper sublevels. (The common lower level plays the role of the virtual level and its decay rate does not influence the width of the resonance.) In addition, the real part of H_7 changes sign in the vicinity of $\omega_{+-} - \Delta\nu = \gamma_a(y - \eta = A)$. This is due

to the fact that the induced polarization due to ρ_{+-} contains another atomic response function, which mixes the real and imaginary parts of ρ_{+-}. This behavior does not show up in the total interaction of the two opposite circular waves, however, because a cancellation takes place between H_6 and H_7. As a result the variation of $H_6 + H_7$ with $y - \eta$ is particularly simple, the real part having an essentially Lorentzian shape with a width $2A = \gamma_a/ku$. Although this behavior is apparently present even for intermediate Doppler broadening, it is easiest to show mathematically for a strongly Doppler broadened line. Assuming a, A, $B \ll 1$, expanding to lowest order in these quantities and using the fact that $y - \eta < a$ for any significant contribution, we have

$$H_6 + H_7 = A/[A + i(y - \eta)] \exp(-x_0^2)$$
$$= \gamma_a/[\gamma_a + i(\omega_{+-} - \Delta\nu)]$$
$$\times \exp[-(\omega_0 - \nu_0)^2/(ku)^2], \quad (31)$$

which shows the simple behavior discussed above, with a Gaussian weighting envelope. Similar resonance behavior of the interaction has been obtained using a scalar theory by Javan and Schlossberg,[25] who make use of the extremely small γ_a in the Xe 3.37-μ laser transition to experimentally probe the hyperfine structure of the upper level.[27]

Since the form of our gain equations is identical to those of laser oscillators, it is convenient to use the same terminology as well. The "coupling parameter" is defined by

$$C = \theta_{+-}\theta_{-+}/\beta_+\beta_-, \quad (32)$$

and the coupling is strong or weak according as C is larger or smaller than unity. Loosely put, strong coupling means that the effect of one field on the other is stronger than on itself. The result of strong coupling in an oscillator is a bistable situation in which one of the two modes is suppressed. In a laser amplifier the consequence of C being larger than unity is not exactly the same. In the region where dE/dz appears to become zero or negative Eqs. (29) and (30) are invalid. Although the effective gain of the weaker signal is made smaller by the stronger field, no quenching takes place. Instead, an intensity unbalance between the input fields is amplified. This will be discussed further in II,[21] which contains results valid for arbitrarily strong fields. The coupling between opposite circularly polarized waves for a $J = 1 \rightarrow J = 0$ transition is critical ($C = 1$) if $\omega_{+-} = \Delta\nu$. Otherwise the coupling is weak and there is a tendency in the amplifier for the field intensities to equalize.[28]

---

[26] W. R. Bennett, Jr., Phys. Rev. 126, 580 (1962).

[27] H. R. Schlossberg and A. Javan, Phys. Rev. Letters 17, 1242 (1966).

[28] It has been experimentally observed in a $J = 1 \rightarrow J = 0$ laser oscillator [R. L. Fork, W. J. Tomlinson, and L. J. Heilos, Appl. Phys. Letters 8, 162 (1966)] that the coupling is actually strong if $\omega_{+-} - \Delta\nu$ is zero or small. This has been attributed to collision effects [Phys. Rev. Letters 20, 647 (1968)] which increase the coupling between opposite circularly polarized fields. In other transitions where the coupling is clearly weak or strong the neglecting of collision effects does not result in such differences of behavior.

It is interesting to note that with y or η (ω_{+-} or $\Delta\nu$) as the independent variable the real and imaginary parts of H_6 and H_7 are related to each other by the Kramers-Kronig relations but those of the self-saturation function H_1 are not. On the other hand, with x_0 as the independent variable, the Kramers-Kronig relations hold for all three functions.

B. Two Signals of Arbitrary Polarizations

The induced polarizations are given by Eqs. (9) and (10). The characteristics and physical significances of the additional functions (H_i, U_i) will now be described.

H_2 describes the common level mutual saturation interaction between the $-$ and the $+$ components of one linearly polarized wave (ν_1), and H_3 is the contribution of the corresponding double quantum interaction of the atoms. Accordingly, the properties of these functions are those of H_6 and H_7, respectively, but with $y-\eta$ replaced by y (since the left and right circular components have the same frequency) and x_0 replaced by $x_0-\eta$ (since $x_0-\eta$ is the detuning of the frequency ν_1 from line center).

H_4 is a new term, caused by the competition for the same population inversion by two different fields of the same polarization. Thus, it has an equivalent in the scalar theory of Lamb[3] and others.[4,7,8] In terms of hole burning, the two fields interact if the two holes, burned by them in the gain curve of the same polarization, overlap. H_4 thus has a width of $2a=2\gamma_{ab}/ku$ about $\eta=0$. In addition, since the center of the transition is given by $x_0+y=0$, a dependence on x_0+y can be observed with a width equal to the Doppler width. Since the same transition is involved, the magnitude of the interaction is independent of the relative size of the decay rates.

The function H_5 also describes an interaction not previously discussed, although a parallel exists in scalar theories. It results from the coherent modulation of the population inversion density by the two fields, at the difference frequency $\Delta\nu=\nu_1-\nu_2$, which gives rise to "sideband" generation. Two of the sidebands coincide with the original frequencies and contribute to the gain and phase correction of the input fields. The important characteristic of this term is the factor $[(A-i\eta)^{-1}+(B-i\eta)^{-1}]$ which causes it to decrease as η becomes larger than A and B (i.e., $\Delta\nu > \gamma_a$, γ_b). Physically, this is due to the fact that only when the frequency difference is smaller than the decay rates is the population inversion capable of following the pulsations of the field. As expected a Doppler variation with x_0+y, identical to that of H_4, is also present.

H_8 and H_9 are the contributions resulting from the interaction of three field components to the induced polarization of the fourth (e.g., of E_{1+}, E_{2-}, and E_{2+} to P_{1-}). These functions contain a multiplying factor dependent on the phase difference of the circularly polarized components. These are the terms that deter-

mine the dependence of the interaction on the polarization characteristics of the input fields. H_8 is a "sideband" term somewhat more complicated than H_5. The modulation of the common-level population by two field components of a given circular polarization [E_{1+} and E_{2+} for the case described by (21)] induces a sideband with the opposite circular polarization ($-$) at the input frequency (ν_1). Accordingly, the characteristics of both the common-level mutual saturation (H_6) and of "sideband" terms (H_5) appear together in H_8. The interaction is proportional to the ratio $\gamma_a/2\gamma_{ab}$ (i.e., it is small when the decay rate γ_b is large) and has the characteristic dependence on ($\omega_{+-}-\Delta\nu$) shown by the multiplicative factor $[a+i(y-\eta)]^{-1}$ appearing in the second and significant term. In addition, however, it contains the factor $(B-i\eta)^{-1}$. Because of this factor, H_8 is significant only if the common-level population is following the pulsations of the field. The composite dependence on the two variables y, η is rather complicated. It is evident that the magnetic field must be small, for otherwise y is large and the conditions $y-\eta=0$ and $\eta=0$ cannot be fulfilled simultaneously.

The last term H_9 complements H_8; it is proportional to γ_b/γ_{ab}. It can be described as follows. The interaction of the atom with both fields E_{2+} and E_{2-} produces a coherence between the upper sublevels. The resulting ρ_{+-} contributes to the polarization at P_{1-} by another interaction of the atom with E_{1+}. For the double quantum interaction, the Raman condition $\omega_{+-}=0$ ($y=0$) has to be satisfied. (The condition is as shown, since $\nu_{+}-\nu_{-}=\nu_2-\nu_2=0$.) Since the lower level acts as a virtual level, the width of this resonance is γ_a. The additional condition that $\nu_1-\nu_2=\omega_{+-}(y-\eta=0)$ must also be fulfilled for ρ_{+-} to contribute to P_{1-}, the width here being the natural linewidth. The resulting final dependence on y and η is again complex, as it was for H_8. The frequency separation must be small to satisfy both $y=0$ and $y=\eta$. A Doppler variation with x_0 is also present in both H_8 and H_9.

Finally we note that for strong Doppler broadening ($a=\gamma_{ab}/ku\rightarrow0$) and the limiting case of $\omega_0-\nu_0=0$, $\omega_{+-}=0$, and $\Delta\nu\rightarrow0$ we have $H_1=H_4=H_5=1$, $H_2=H_6=H_8=A/a=\gamma_a/2\gamma_{ab}$, and $H_3=H_7=H_9=B/a=\gamma_b/2\gamma_{ab}$, while for natural broadening ($a=\gamma_{ab}/ku\rightarrow\infty$) the functions have twice the above values, provided we replace a by α_0.

The functions U_i, appearing in the "sideband" components of the polarization, are closely related to the saturation functions. Briefly, U_1 corresponds to H_5 and is caused by direct modulation of a given population inversion; U_2 corresponds to H_8 and is due to the modulation of the common-level population; U_3 corresponds to H_9 and results from the coherent interaction of two field components of opposite circular polarizations. Since the induced polarization contains frequency components not present in the input, the form assumed for the field is obviously not correct. The new components must also be included. These can cause nonlinear saturation and induce still new fields. Exact
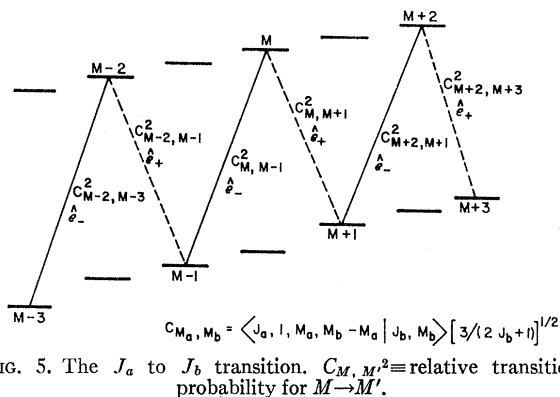
$$C_{M_a, M_b} = \langle J_a, 1, M_a, M_b - M_a \mid J_b, M_b \rangle [3/(2J_b+1)]^{1/2}$$

FIG. 5. The J_a to J_b transition. $C_{M,M'}{}^2 \equiv$ relative transition probability for $M \to M'$.

treatment of the problem would require an infinite set of nonlinear equations. In practice, however, the combination-tone fields are small and any nonlinear effects caused by them may safely be neglected. Equations (28a) and (28b) can thus still be used for the input fields with either time or space derivatives set equal to zero, while the combination-tone fields require separate treatment.

Further discussion of the nonlinear behavior of the laser amplifier is postponed until the results for the general J_a to J_b transition are derived.

4. J_a TO J_b TRANSITION

Mathematically, the calculations for this general case proceed as for the $J=1 \to J=0$ model. The results, while appearing quite complex, can be interpreted in terms of the same nonlinear interactions that take place in the simple $J=1 \to J=0$ model and were discussed in some detail in Sec. 3.

A typical portion of a $J_a \to J_b$ transition is shown in Fig. 5. The gain due to the $M \to M-1$ transition is saturated by the nonlinear interactions with the same

transition, described by the functions H_1, H_4, and H_5. In addition, cross saturations (with opposite circularly polarized components) are present due to the $M-2 \to M-1$ and the $M \to M+1$ transitions, each of which has a common level with $M \to M-1$. The first of these introduces the nonlinear functions H_2, H_3, and H_6 to H_9 while the latter adds a similar set in which the roles of the a and b levels are reversed. In the results that follow the superscript a indicates that the twin sublevels $(M, M-2)$ are in a and the common level $(M-1)$ is in b while b indicates twin sublevels in b $(M-1, M+1)$ and a common level in a (M). Unlike in the $J=1 \to J=0$ model, the transition probabilities are in general unequal and the contribution of each transition is weighted by its relative strength. Since there may be different Zeeman splitting in the lower and upper levels, the arguments of the nonlinear functions differ slightly from those in Sec. 3 and may be different for each sublevel. An additional subscript M shall designate the functions saturating the transition which originates on the M upper level. Defining

$$y^a = \omega_{a,a,M,M-2}/2ku, \tag{33}$$

$$y^b = \omega_{b,b\,M,M-2}/2ku, \tag{34}$$

$$\delta = y^a - y^b, \tag{35}$$

the new nonlinear functions are found by

$H_j \to H_{jM}$ replace x_0 by $x_0 + M\delta$ and y by y^b or, equivalently,

       replace x_0 by $x_0 + (M-1)\delta$ and y by y^a;

$H_j \to H_{jM}{}^a$ replace x_0 by $x_0 + (M-1)\delta$ and y by y^a;

$H_j \to H_{jM}{}^b$ replace x_0 by $x_0 + M\delta$ and y by y^b, and interchange A and B.

The circularly polarized component $\mathcal{P}_{1-}$ is given by

$$(\nu/2\epsilon_0 c)\mathcal{P}_{1-} = -i\alpha E_{1-} \sum_M C_{M,M-1}{}^2 \{\omega^*(x_0 + M\delta + y^b + ia) - (E_{1-}{}^2/2E_0{}^2)C_{M,M-1}{}^2 H_{1M}$$

$$- (E_{1+}{}^2/2E_0{}^2)[C_{M-2,M-1}{}^2(H_{2M}{}^a + H_{3M}{}^a) + C_{M,M+1}{}^2(H_{2M}{}^b + H_{3M}{}^b)] - (E_{2-}{}^2/2E_0{}^2)C_{M,M-1}{}^2(H_{4M} + H_{5M})$$

$$- (E_{2-}{}^2/2E_0{}^2)[C_{M-2,M-1}{}^2(H_{6M}{}^a + H_{7M}{}^a) + C_{M,M+1}{}^2(H_{6M}{}^b + H_{7M}{}^b)]\}$$

$$+ i\alpha(E_{1+}E_2 - E_{2+}/2E_0{}^2) \sum_M C_{M,M-1}{}^2[C_{M-2,M-1}{}^2(H_{8M}{}^a + H_{9M}{}^a) + C_{M,M+1}{}^2(H_{8M}{}^b + H_{9M}{}^b)]. \tag{36}$$

In the above,

$$C_{M,M'}{}^2 = [3/(2J_b+1)][\langle J_a, 1, M, m \mid J_b, M' \rangle]^2,$$

where $m = M' - M$, and the summation runs over all M values of the upper (a) level. $\mathcal{P}_{1+}$, $\mathcal{P}_{2-}$, and $\mathcal{P}_{2+}$ are given by similar equations. To obtain $\mathcal{P}_{j+}$ from $\mathcal{P}_{j-}$ interchange $+$ and $-$ subscripts and replace y^a, y^b, δ, and M by $-y^a$, $-y^b$, $-\delta$, $-M$. To obtain $\mathcal{P}_{2m}$ from $\mathcal{P}_{1m}$ interchange 1 and 2 subscripts and replace η by $-\eta$.

Similarly, the induced polarization at the new frequency $\nu_0 = 2\nu_1 - \nu_2$ is

$$(\nu/2\epsilon_0 c)\mathcal{P}_{0-} = i\alpha E_{1-} \sum_M C_{M,M-1}{}^2$$

$$\times \{(E_1 - E_2 - /2E_0{}^2)C_{M,M-1}{}^2 U_{1M}$$

$$+ (E_{1+}E_{2+}/2E_0{}^2)[C_{M-2,M-1}{}^2(U_{2M}{}^a + U_{3M}{}^a)$$

$$+ C_{M,M+1}{}^2(U_{2M}{}^b + U_{3M}{}^b)]\exp(i2\theta)\}, \tag{37}$$

where the same rules apply to the U_{jM}'s as to the H_{jM}'s.

TABLE I. The Clebsch-Gordan coefficient combinations determining interaction strength and combination-tone generation.

J_a	$\frac{1}{2}$	1	1	$\frac{3}{2}$	$\frac{3}{2}$	2	2	$\frac{5}{2}$	$\frac{5}{2}$	3	3	$\frac{7}{2}$	$\frac{7}{2}$	4	4	J_b
J_b	$\frac{1}{2}$	0	1	$\frac{1}{2}$	$\frac{3}{2}$	1	2	$\frac{3}{2}$	$\frac{5}{2}$	2	3	$\frac{5}{2}$	$\frac{7}{2}$	3	4	J_a
C_2	0	1	$\frac{1}{4}$	$\frac{3}{8}$	$\frac{12}{50}$	$\frac{21}{100}$	$\frac{21}{100}$	$\frac{28}{200}$	$\frac{32}{175}$	$\frac{18}{175}$	$\frac{9}{56}$	$\frac{18}{224}$	$\frac{12}{84}$	$\frac{11}{168}$	$\frac{77}{600}$	C_3
C_3	0	0	$\frac{1}{4}$	0	$\frac{12}{50}$	$\frac{1}{100}$	$\frac{21}{100}$	$\frac{3}{200}$	$\frac{32}{175}$	$\frac{3}{175}$	$\frac{9}{56}$	$\frac{3}{224}$	$\frac{12}{84}$	$\frac{3}{168}$	$\frac{77}{600}$	C_2
C_2+C_3	0	1	$\frac{1}{2}$	$\frac{3}{8}$	$\frac{24}{50}$	$\frac{22}{100}$	$\frac{42}{100}$	$\frac{31}{200}$	$\frac{64}{175}$	$\frac{21}{175}$	$\frac{18}{56}$	$\frac{21}{224}$	$\frac{24}{84}$	$\frac{14}{168}$	$\frac{154}{600}$	C_2+C_3
C_1	1	1	$\frac{1}{2}$	$\frac{5}{8}$	$\frac{17}{50}$	$\frac{46}{100}$	$\frac{26}{100}$	$\frac{73}{200}$	$\frac{37}{175}$	$\frac{53}{175}$	$\frac{10}{56}$	$\frac{58}{224}$	$\frac{13}{84}$	$\frac{38}{168}$	$\frac{82}{600}$	C_1
$|C_1-(C_2+C_3)|$	1	0	0	$\frac{2}{8}$	$\frac{7}{50}$	$\frac{24}{100}$	$\frac{16}{100}$	$\frac{42}{200}$	$\frac{27}{175}$	$\frac{32}{175}$	$\frac{8}{56}$	$\frac{37}{224}$	$\frac{11}{84}$	$\frac{24}{168}$	$\frac{72}{600}$	$|C_1-(C_2+C_3)|$

A. Two Circularly Polarized Signals

Only H_{1M}, $H_{6M}{}^a$, $H_{6M}{}^b$, $H_{7M}{}^a$, $H_{7M}{}^b$ appear in the induced polarization. For strong Doppler broadening these become

$$H_{1M} \rightarrow \exp-[x_0+y^b+M\delta-\eta]^2$$
$$= \exp-[(\omega_{a,b,M,M-1}-\nu_{1-})/ku]^2, \quad (38a)$$

$$H_{6M}{}^a+H_{7M}{}^a \rightarrow A[A+i(y^a-\eta)]^{-1}$$
$$\times \exp-[x_0+(M-1)\delta]^2, \quad (38b)$$

$$H_{6M}{}^b+H_{7M}{}^b \rightarrow B[B+i(y^b-\eta)]^{-1} \exp-[x_0+M\delta]^2. \quad (38c)$$

The nonlinear coefficients are

$$\beta_- = (\alpha/2E_0{}^2) \, \mathrm{Re} \sum_M C_{M,M-1}{}^4 H_{1M}, \quad (39a)$$

$$\theta_{-+} = (\alpha/2E_0{}^2) \, \mathrm{Re}[\sum_M C_{M,M-1}{}^2 C_{M-2,M-1}{}^2 (H_{6M}{}^a+H_{7M}{}^a)$$
$$+ \sum_M C_{M,M-1}{}^2 C_{M,M+1}{}^2 (H_{6M}{}^b+H_{7M}{}^b)], \quad (39b)$$

$$\rho_- = (\alpha/2E_0{}^2) \, \mathrm{Im} \sum_M C_{M,M-1}{}^4 H_{1M}, \quad (39c)$$

$$\tau_{-+} = (\alpha/2E_0{}^2) \, \mathrm{Im}[\sum_M C_{M,M-1}{}^2 C_{M-2,M-1}{}^2 (H_{6M}{}^a+H_{7M}{}^a)$$
$$+ \sum_M C_{M,M-1}{}^2 C_{M,M+1}{}^2 (H_{6M}{}^b+H_{7M}{}^b)]. \quad (39d)$$

For the corresponding coefficients with $+$ and $-$ subscripts interchanged we replace y^a, y^b, δ, η, and M by their negatives.

The strength of the interaction between the two fields is determined by the two Lorentzians[29] and by the constants $C_{M,M'}{}^2$. Evidently, in zero or small magnetic field and small frequency separation the coupling between the circularly polarized signals is strong when

$$\sum_M [C_{M,M-1}{}^2 C_{M-2,M-1}{}^2 + C_{M,M-1}{}^2 C_{M,M+1}{}^2] > \sum_M C_{M,M-1}{}^4$$

or

$$C_2+C_3 > C_1, \quad (40)$$

and weak when the inequality is reversed. The values of these coefficients are tabulated in Table I. It is seen that, with the exception of the $J=1 \rightarrow J=1$ transition, strong coupling occurs whenever $\Delta J = 0$. Since $C_2 = C_3$ for $\Delta J = 0$, the region of strong coupling in zero magnetic field is determined by the condition

$$\gamma_a{}^2[\gamma_a{}^2+(\Delta\nu)^2]^{-1}+\gamma_b{}^2[\gamma_b{}^2+(\Delta\nu)^2]^{-1} > C_2/C_1. \quad (41)$$

For large magnetic fields, because the g factors are usually unequal, the two resonances do not coincide. Although there are peaks in the interaction ("dips" in the gain) where the Zeeman splitting of the upper or lower levels equal $\Delta\nu$, the coupling remains weak. For $\Delta\nu = 0$ (single, linearly polarized signal) and near zero magnetic field, our results agree with those of Heer and Graft,[16] who did not, however, calculate the frequency and magnetic field dependence of this effect. Figure 6 shows the variation of the coupling coefficient C with frequency and magnetic field for various transitions. These may be compared with the corresponding curves of Sargent, Lamb, and Fork[19] for oscillators.

---

[29] By Lorentzian we mean, in the broader sense, a function of the form $\gamma(\gamma+ix)^{-1}$ whose real part represents a Lorentzian line shape.
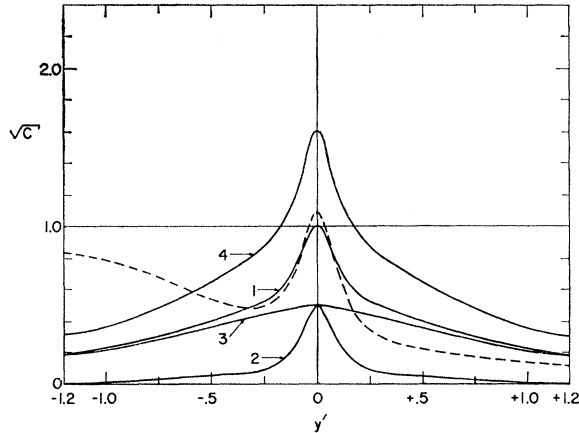
FIG. 6. The coupling coefficient $\sqrt{C}$ versus frequency or magnetic field for two circularly polarized signals and strong Doppler broadening; $\gamma_a=0.2\gamma_{ab}$, $\gamma_b=1.8\gamma_{ab}$. Solid lines: *either* g factors are equal and $y'=(\omega_{+-}-\Delta\nu)/2\gamma_{ab}$ or $\omega_{+-}=0$ and $y'=\Delta\nu/2\gamma_{ab}$. (1) $J=1\rightarrow J=1$, (2) $J=2\rightarrow J=1$, (3) $J=1\rightarrow J=2$, (4) $J=2\rightarrow J=2$. Dashed line: $J=2\rightarrow2$, $y'=(\omega_{+-}{}^a-\Delta\nu)/2\gamma_{ab}$, $\omega_{+-}{}^b-\omega_{+-}{}^a=1.2\gamma_{ab}$.

It is well known that for $\Delta J=\pm1$ the outer transitions (e.g., $M_a=J_a\rightarrow M_b=J_b$) are strong and the inner transitions (e.g., $M_a=J_a\rightarrow M_b=J_b-2$) are weak because of good and poor overlap of the electron distributions, respectively. This unequal distribution of the transition probabilities results in weak coupling, as it is shown in a simplified form in Fig. 7. Most of the gain is contributed by the $M=\pm1\rightarrow M=\pm2$ transitions which are very weakly saturated by their neighbors. For $\Delta J=0$, on the other hand, the transition probabilities are more evenly distributed, resulting in strong coupling.

For the special case of a single elliptically polarized signal in zero magnetic field, the effect of weak or strong coupling can be more readily seen by recasting the gain equations into an equation for the ellipticity and another for the total intensity. Defining $r=(E_--E_+)/(E_-+E_+)$ and $E^2=E_-^2+E_+^2$, we obtain

$$\frac{dr}{dz}=-\alpha r\,\frac{E^2}{2E_0^2}\,\frac{1-r^2}{1+r^2}\,(C_1-C_2-C_3)\,\mathrm{Re}H_1(x_0,0,0),$$

(42a)

$$\frac{dE}{dz}=\alpha E\left\{\mathrm{Re}w^*(x_0+ia)-\frac{E^2}{2E_0^2}\right.$$

$$\left.\times\left[C_1+\tfrac12(C_2+C_3-C_1)\,\frac{1-r^2}{1+r^2}\right]\mathrm{Re}H_1(x_0,0,0)\right\}.\quad(42b)$$

It is seen that r increases for strong and decreases for weak coupling of the circularly polarized components. Equation (42a) is analogous to one obtained by Polder and Van Haeringen[17] for oscillators.

For two signals of arbitrary polarization the four field components must, in general, be treated separately. This results in eight nonlinear equations in which the

coefficients are determined by the functions H_{jM}. Equation (13) can be used to calculate these coefficients for any specific case. In the next section the special case of zero magnetic field is discussed in more detail.

B. Two Elliptically Polarized Fields. Zero Magnetic Field

We define two complex unit vectors $\hat{e}_1$ and $\hat{e}_2$ by

$$\hat{e}_1=a_{1-}\hat{e}_-+a_{1+}\hat{e}_+,\qquad(43\text{a})$$

$$\hat{e}_2=a_{2-}\hat{e}_-+a_{2+}\hat{e}_+,\qquad(43\text{b})$$
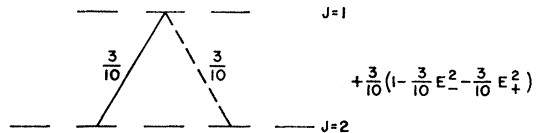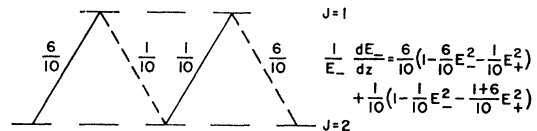
where $a_{j\pm}=E_{j\pm}/(E_{j+}{}^2+E_{j-}{}^2)^{1/2}$. The electromagnetic field then can be written as

$$\mathbf{E}(z,t)=\mathrm{Re}\{\hat{e}_1E_1\exp i(k_1z-\nu_1t+\phi_1)$$

$$+\hat{e}_2E_2\exp i(k_2z-\nu_2t+\phi_2)\}.\quad(44)$$

We can calculate the components of the induced polarization along $\hat{e}_1$ and $\hat{e}_2$ and thus find the incremental gain and phase change for each field. Other pertinent parameters are

$$r_j=(E_j-E_{j+})/(E_{j-}+E_{j+}),\qquad(45)$$

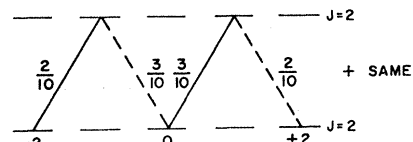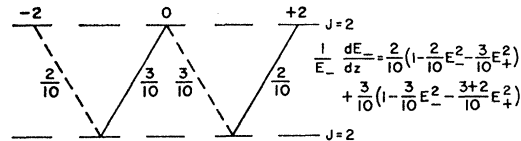$\Delta J=+1$. WEAK COUPLING

$\Delta J=0$. STRONG COUPLING

FIG. 7. A simple description of weak and strong coupling.

the ratio of the minor to the major axis and θ, the angle between the major axes which has been defined in Sec. 3. Since the magnetic sublevels are identical, after some simple algebra we have

$$(\nu/2\epsilon_0 c)\mathcal{P}_1 = -i\alpha E_1\{w^*(x_0-\eta+ia)-(E_1{}^2/2E_0{}^2)R_1 f_1(x_0,\eta)$$

$$-(E_2{}^2/2E_0{}^2)[R_2 f_2(x_0,\eta)+R_3 f_3(x_0,\eta)]\}, \quad (46)$$

where

$$R_1 = C_1 + \tfrac{1}{2}(C_2+C_3-C_1)\left(\frac{1-r_1{}^2}{1+r_1{}^2}\right)^2, \quad (47a)$$

$$R_2 = C_2 + \frac{1}{2}\frac{1-r_1{}^2}{1+r_1{}^2}\frac{1-r_2{}^2}{1+r_2{}^2}C_3\cos2\theta$$

$$+\frac{1}{4}\frac{(1+r_1)^2(1+r_2)^2+(1-r_1)^2(1-r_2)^2}{(1+r_1{}^2)(1+r_2{}^2)}(C_1-C_2), \quad (47b)$$

$$R_3 = C_3 + \frac{1}{2}\frac{1-r_1{}^2}{1+r_1{}^2}\frac{1-r_2{}^2}{1+r_2{}^2}C_2\cos2\theta$$

$$+\frac{1}{4}\frac{(1+r_1)^2(1+r_2)^2+(1-r_1)^2(1-r_2)^2}{(1+r_1{}^2)(1+r_2{}^2)}(C_1-C_3), \quad (47c)$$

and a similar equation for $\mathcal{P}_2$. The frequency-dependent functions are

$$f_1(x_0,\eta) = H_1(x_0,0,\eta)$$

$$\rightarrow\exp(-x_0{}^2) = \exp-[(\omega_0-\nu_0)/ku]^2, \quad (48a)$$

$$f_2(x_0,\eta) = H_6(x_0,0,\eta)+H_7(x_0,0,\eta)$$

$$\rightarrow\gamma_a(\gamma_a-i\Delta\nu)^{-1}\exp(-x_0{}^2), \quad (48b)$$

$$f_3(x_0,\eta) = f_2(x_0,\eta; A\rightleftarrows B)$$

$$\rightarrow\gamma_b(\gamma_b-i\Delta\nu)^{-1}\exp(-x_0{}^2). \quad (48c)$$

The arrows indicate the behavior for strong Doppler broadening. When $\mathcal{P}_1$ and $\mathcal{P}_2$ are substituted into Maxwell's equations (ignoring the new frequency components $\mathcal{P}_0$ and $\mathcal{P}_3$, as discussed), gain and phase equations identical with (29a)–(29d) are obtained (with subscripts 1 and 2 replacing $+$ and $-$). The nonlinear coefficients are

$$\beta_1 = (\alpha/2E_0{}^2)R_1\operatorname{Re}f_1(x_0,\eta), \quad (49a)$$

$$\theta_{12} = (\alpha/2E_0{}^2)[R_2\operatorname{Re}f_2(x_0,\eta)+R_3\operatorname{Re}f_3(x_0,\eta)], \quad (49b)$$

$$\rho_1 = (\alpha/2E_0{}^2)R_1\operatorname{Im}f_1(x_0,\eta), \quad (49c)$$

$$\tau_{12} = (\alpha/2E_0{}^2)[R_2\operatorname{Im}f_2(x_0,\eta)+R_3\operatorname{Im}f_3(x_0,\eta)]. \quad (49d)$$

For the corresponding coefficients with subscripts 1 and 2 reversed η is replaced by $-\eta$ and r_1 and r_2 are

interchanged. These results may be compared with those of Doyle and White[18] for oscillators.

From the definition of r_1 and Eq. (36) one has

$$\frac{dr_1}{dz} = -\alpha(1-r_1{}^2)\left\{\frac{E_1{}^2}{4E_0{}^2}\frac{2r_1}{1+r_1{}^2}(C_1-C_2-C_3)\operatorname{Re}f_1(x_0,\eta)\right.$$

$$+\frac{E_2{}^2}{4E_0{}^2}\frac{2r_2}{1+r_2{}^2}[C_1\operatorname{Re}(f_2+f_3)-C_2\operatorname{Re}f_2-C_3\operatorname{Re}f_3]$$

$$\left.-\frac{E_2{}^2}{4E_0{}^2}\frac{1-r_2{}^2}{1+r_2{}^2}[C_2\operatorname{Im}f_3+C_3\operatorname{Im}f_2]\sin2\theta\right\}, \quad (50)$$

with a similar equation for dr_2/dz. The final equation is that for θ which will be given only for those cases when $f_i(x_0,\eta)=f_i{}^*(x_0,-\eta)$ (either $x_0=0$ or strong Doppler broadening). Then,

$$\frac{d\theta}{dz} = \alpha\left\{\frac{2r_1}{1+r_1{}^2}\frac{E_1{}^2-E_2{}^2}{4E_0{}^2}[(C_1-C_2-C_3)\operatorname{Im}f_1(x_0,\eta)\right.$$

$$+C_1\operatorname{Im}(f_2+f_3)-C_2\operatorname{Im}f_2-C_3\operatorname{Im}f_3]$$

$$\left.+\frac{E_1{}^2+E_2{}^2}{4E_0{}^2}[C_2\operatorname{Re}f_3+C_3\operatorname{Re}f_2]\sin2\theta\right\}. \quad (51)$$

The above suggest the existence of various nonlinearity induced anisotropies. The only stable equilibrium (isotropy) is for two perpendicular linear fields. Parallel polarized fields are in unstable equilibrium. Other linear and all elliptical polarizations are not in equilibrium. For small frequency separation of linearly polarized signals, dr_j/dz is approximately zero, i.e., the polarizations remain linear. Then the relative orientation change is

$$\frac{d\theta}{dz} = \alpha\frac{E_1{}^2+E_2{}^2}{4E_0{}^2}(C_2\operatorname{Re}f_3+C_3\operatorname{Re}f_2)\sin2\theta, \quad (52)$$

which indicates that the polarizations will rotate apart. The coupling of E_1 and E_2 will be discussed by further specializing to two identical, two arbitrary linear, and two orthogonal elliptical polarizations.

a. Two Identically Polarized Signals

For this case, $\theta=0$ and $r_1=r_2$, and R_2, R_3 become identical with R_1. Then

$$C = (\operatorname{Re}(f_2+f_3)/\operatorname{Re}f_1)^2, \quad (53)$$

which is the same as the result of the scalar theory.[7] C is maximum for $\Delta\nu=0$ and is equal to 4.

b. Linearly Polarized Signals

Since $r_1=r_2=0$, the results simplify considerably. If in addition strong Doppler broadening is assumed, the coupling coefficient is

$$C = \left[\frac{(C_1+C_2+C_3\cos2\theta)[\gamma_a{}^2/(\gamma_a{}^2+(\Delta\nu)^2)]+(C_1+C_3+C_2\cos2\theta)[\gamma_b{}^2/(\gamma_b{}^2+(\Delta\nu)^2)]}{C_1+C_2+C_3}\right]^2. \quad (54)$$

For small frequency separation, $\Delta\nu\ll\gamma_a$, γ_b, this becomes

$$C=\left(\frac{2C_1+2(C_2+C_3)\,\cos^2\theta}{C_1+C_2+C_3}\right)^2.\quad(55)$$

For parallel polarization of the input signals ($\theta=0$) the coupling is strong, $C=4$. For perpendicular polarization the interaction depends on ΔJ. If $\Delta J=1$, $\theta_{12}>\beta_1$ (strong coupling), while if $\Delta J=0$, $\theta_{12}<\beta_1$ (weak coupling). This is the reverse of the situation for opposite circularly polarized fields. The $J=1\rightleftarrows J=0$ transitions, however, are special cases and give critical coupling.

For arbitrary frequency separation and angle θ the region of strong coupling can be determined by Eq. (51). Figure 8 shows the coupling coefficient C versus $\Delta\nu$. The results of this section have been used in another paper[30] to investigate the validity and significance of the two nondegenerate levels model in nonlinear vector-field calculations.

c. Orthogonal Elliptical Signals

For this case $r_1=-r_2$ and $\theta=\frac{1}{2}\pi$. The coupling coefficient for strong Doppler broadening is

$$C=\left[\frac{[0.5p^2(C_1-C_2-C_3)+C_2][\gamma_a^2/(\gamma_a^2+(\Delta\nu)^2)]+[0.5p^2(C_1-C_2-C_3)+C_3][\gamma_b^2/(\gamma_b^2+(\Delta\nu)^2)]}{C_1+0.5p^2(C_2+C_3-C_1)}\right]^2,\quad(56)$$

where $p=(1-r^2)/(1+r^2)$. For $\Delta\nu\ll\gamma_a$, γ_b

$$C=\left[\frac{p^2(C_1-C_2-C_3)+C_2+C_3}{C_1+0.5p^2(C_2+C_3-C_1)}\right].\quad(57)$$

Figure 9 shows the variation of C with the ellipticity. It reveals the remarkable fact that for $\Delta\nu\ll\gamma_a$, γ_b critical coupling occurs at the same eccentricity, independent of the J values. From Eq. (57) we find $r_{\rm crit}=0.319$.

C. Combination Tones

Combination-tone generation for two arbitrarily polarized signals and nonzero magnetic field has been considered in an earlier paper.[20] Here we shall examine in more detail the generation of new fields for zero magnetic field and two elliptically polarized signals of the same eccentricity and opposite sense of rotation. Noting that for zero magnetic field $U_{2M}{}^a+U_{3M}{}^a=U_{2M}{}^b+U_{3M}{}^b=U_1$, one has

$$(\nu/2\epsilon_0 c)\,\mathcal{P}_{0\mp}=i\alpha\{E_{2\pm}(E_1{}^2/2E_0{}^2)[(1-r^2)/(1+r^2)]$$

$$\times[C_1+(C_2+C_3)e^{\pm i2\theta}]U_1(x_0,0,\eta)\}$$

$$\times\exp[i(2\varphi_{1\mp}-\varphi_{2\mp})].\quad(58)$$

The phase angle of the bracketed quantity is $\pm\phi'$, where

$$\phi'=\tan^{-1}\frac{(C_2+C_3)\,\sin2\theta}{C_1+(C_2+C_3)\,\cos2\theta}.\quad(59)$$

Thus $\mathcal{P}_{0\mp}$ is

$$(\nu/2\epsilon_0 c)\,\mathcal{P}_{0\mp}=i\alpha\{E_{2\pm}(E_1{}^2/2E_0{}^2)[(1-r^2)/(1+r^2)]$$

$$\times[C_1{}^2+(C_2+C_3)^2+C_1(C_2+C_3)\,\cos2\theta]^{1/2}\}$$

$$\times U_1(x_0,0,\eta)\,\exp(i\varphi_{0\mp}),\quad(60)$$

where $\phi_{0\mp}=2\phi_{1\mp}-\phi_{2\mp}\pm\phi'$. We can now find the polarization of the combination tone at ν_0. Since there is no field originally at ν_0 it builds up $90°$ out of phase with $\mathcal{P}_0$. It is evident that $\mathcal{P}_0$ is elliptically polarized with eccentricity and sense of rotation the same as E_1. The

direction of the major axis is

$$\Phi_0=\frac{1}{2}(\phi_{0-}-\phi_{0+})=2\Phi_1-\Phi_2+\phi'$$

$$=\Phi_1-\theta+\phi'.\quad(61)$$

The expected polarization patterns are shown on Fig. 10. It is interesting to note that for the $1\rightarrow0$, $0\rightarrow1$, and $1\rightarrow1$ transitions, since $\phi'=\theta$, the polarization of $\mathcal{P}_0$ is identical with that of E_1. For these transitions, however, we also find that $\mathcal{P}_0$ is identically zero for $\theta=90°$, i.e., for orthogonal polarizations of the input fields. This apparent contradiction with the qualitative predictions of Sec. 1 can be explained by the fact that for these (and only for these) transitions there exist orthogonal combinations of the magnetic substates which result in perpendicular linear or orthogonal elliptical transitions. This situation is shown in Fig. 11. In the equally valid representation shown on the right, E_1 and E_2 interact with different transitions, producing
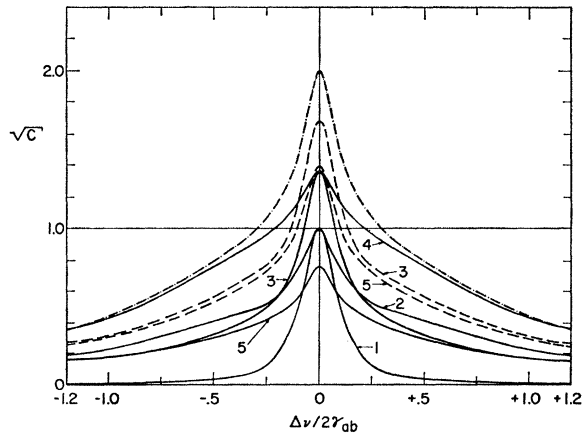

Fig. 8. The coupling coefficient $\sqrt{C}$ versus $\Delta\nu$ for two linearly polarized signals. Strong Doppler broadening, $\gamma_a=0.2\gamma_{ab}$, $\gamma_b=1.8\gamma_{ab}$. (1) $J=1\rightarrow J=0$, (2) $J=1\rightarrow J=1$, (3) $J=2\rightarrow J=1$, (4) $J=1\rightarrow J=2$, (5) $J=2\rightarrow J=2$. Solid: $\theta=90°$, dashed: $\theta=45°$, dash-dot: $\theta=0°$, all transitions.

[30] A. Dienes, IEEE J. Quantum Electron. QE-4, 260 (1968).

no combination tones.[31] For all other J values combination tones are present with polarizations as shown in Fig. 10.[32] For $\theta = 90°$ these are in agreement with the work of Doyle and White.[33]

5. CONCLUSIONS

We have derived equations for the nonlinear behavior of two weak signals in a laser amplifier. The results show a complex dependence on the polarization states, on the J values of the levels, and on various other atomic parameters. We have attempted to explain these in terms of simpler interactions of circularly polarized field components with the corresponding transitions between magnetic sublevels. For full usefulness, it is necessary to investigate the nonlinear behavior of the laser amplifier for arbitrarily strong field intensi-
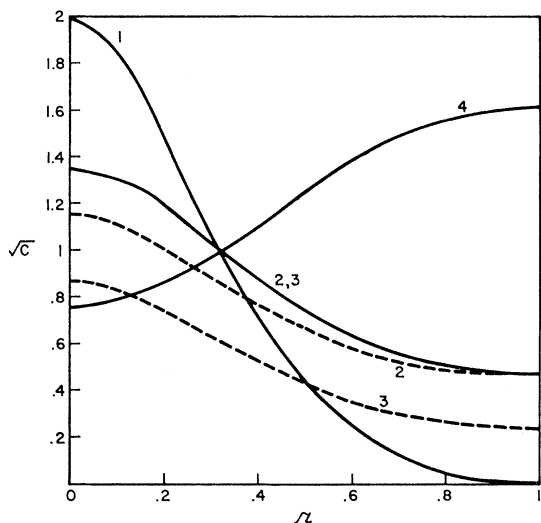

FIG. 10. The predicted polarization pattern for the combination tones.

FIG. 9. The coupling coefficient $\sqrt{C}$ versus ellipticity. (1) $J=\frac{1}{2}\to J=\frac{1}{2}$, (2) $J=1\to J=2$, (3) $J=2\to J=1$, (4) $J=2\to J=2$. Solid: $\Delta\nu=0$, dash: $\Delta\nu=\gamma_a=0.2\gamma_{ab}$.

ties for which the perturbational results of this paper are no longer valid. This is the subject of the following paper.[21]

The results of the previous sections are well suited for the determination of various atomic parameters. Methods utilizing nonlinear wave interactions in amplifiers can, under some circumstances, have advantages over those using the nonlinear properties of laser

oscillators.[34] In particular, measurements can be carried out on a medium with absorption instead of gain. It is necessary only to change the sign of the gain parameter α for our results to be applicable. Also, the experimental results are not complicated by the presence of the cavity.

While in laser oscillator experiments[35] the atomic parameters are extracted from observations of the output intensity, in amplifier (or absorber) experiments it is most convenient to observe directly the dependence of the coefficient θ_{12} on some convenient parameter by detecting the effect of one signal on the other. The quantity θ_{12} is almost identical to $\sqrt{C}$, shown in Figs. 6, 8, and 9 (for zero detuning they become identical). Such an experiment has been recently performed by Shank and Schwarz[36] with parallel linearly polarized waves [this is a special case of Eq. (49b)], who measured in this manner the natural width of the 6328 Å Ne line in both He–Ne (population inverted) and pure Ne (passive) discharges. By performing similar measurements for perpendicularly polarized

$$\vec{E}=\vec{E}_X(\nu_1)+\vec{E}_Y(\nu_2)$$

FIG. 11. The physical reason for the lack of combination tones for orthogonal polarized fields in the $J=1\to0$ transition.

---

[31] This picture is of course only valid for completely degenerate levels. In nonzero magnetic field the U_{jM}'s are not equal and the cancellation does not take place. Combination tones appear as soon as the sublevels are separated beyond their natural width. Results showing this have been graphically presented in Ref. 20.

[32] We do not attempt to calculate the growth of the combination-tone fields but only find the magnitude and polarization characteristics of the induced polarization at the new frequencies.

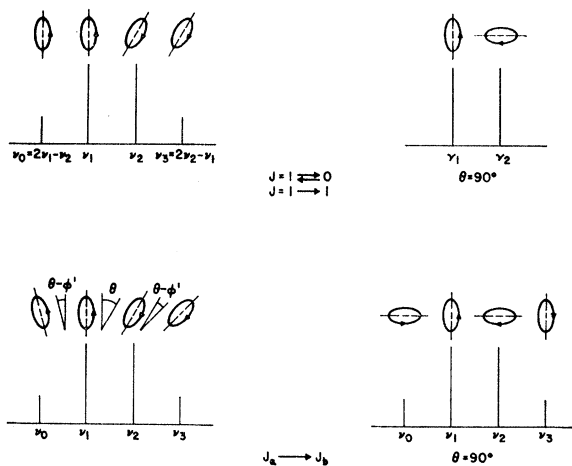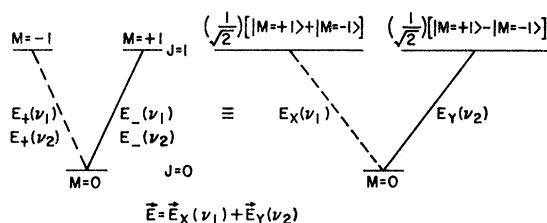[33] W. M. Doyle and M. B. White, Appl. Phys. Letters **10**, 224 (1967).

[34] Section VIII of Ref. 19 describes how atomic constants may be found by laser oscillator experiments. See also W. J. Tomlinson and R. L. Fork, Phys. Rev. **164**, 466 (1967); and Ref. 27.

[35] θ_{12} is a meaningful quantity only in low-gain amplifiers, with weak saturation effects. Possible measurements in high gain, strongly saturated media will be briefly discussed in II.

[36] C. V. Shank and S. E. Schwarz, Appl. Phys. Letters (to be published).

waves (see Fig. 8) the individual decay rates γ_a and γ_b can also be extracted.

Measuring the variation of θ_{12} with the angle between the polarization vectors provides a way of identifying the J values of the levels as well. This curve is unique for any given pair of J values and is easiest to interpret if $\nu_1 = \nu_2$.[37] The g factors of the levels can also be found conveniently using two circularly polarized input fields, and applying an axial magnetic field on the amplifier. The relevant curves here are similar to the dashed curve of Fig. 6. This experiment separates the resonances due to the lower and upper levels and thus serves also to determine γ_a and γ_b.

As it is indicated by Eqs. (28a) and (28b) any of the gain and phase equations in this paper may be

transformed into ones for a ring laser (with fields circulating in one direction) by carrying out the following changes:

$$dE_j/dz \rightarrow c^{-1}dE_j/dt + 0.5(Q_j\lambda_j)^{-1},$$

$$d\phi_j/dz \rightarrow c^{-1}(\nu_j - \Omega_j).$$

The steady-state oscillation solutions then are found by setting $dE_j/dt = 0$ exactly in the manner of Sargent, Lamb, and Fork.[19] These authors have discussed the possible forms and useful transformations of the cavity loss matrix Q.

ACKNOWLEDGMENTS

---

[37] This curve has been measured recently for the 6328 Å line. Excellent agreement with the theoretical results was found. C. V. Shank and S. E. Schwarz (to be published).

Theory of Nonlinear Effects in a Gas Laser Amplifier. II. Strong Signals

ANDREW DIENES

Bell Telephone Laboratories, Holmdel, New Jersey

The model given in the preceding paper is used to calculate the nonlinear gain and phase of a laser amplifier operating at field intensities that may be too large for the perterbational results to be valid. The induced polarization is calculated exactly by integrating the macroscopic density-matrix differential equations. The incremental gain and phase shift are found to be complicated functions of the circularly polarized field intensity components. Simple physical interpretations of these functions are given. The results are used to compute the change in the ellipticity of a single-frequency signal in a high-gain amplifier.

1. INTRODUCTION

IN Paper I[1] a weak-signal theory of a laser amplifier was given. In this paper a strong-signal theory is developed by solving the density-matrix equations exactly. Owing to considerable difficulties encountered in obtaining exact solutions, the results presented here are not as general and complete as those of the previous paper. In that paper the polarization of the signals, the frequencies, and all atomic parameters are treated in a general fashion, but the results are limited to weakly saturated signals. In the present paper the results are available only for special cases of polarization, frequencies, and atomic parameters but are valid for arbitrarily strong field intensities. Although we primarily deal with two opposite circularly polarized

signals, in Sec. 4 we briefly discuss linearly polarized signals.

2. SIMPLE TRANSITIONS

Under this heading we include the $J = 1 \rightleftarrows J = 0$, the $J = 1 \rightarrow J = 1$, and the $J = \frac{1}{2} \rightleftarrows J = \frac{3}{2}$ transitions. These are all constituted of noninteracting 3-level subsystems. The density-matrix equations for such a subsystem will now be solved. The equations are the same as for the $J = 0 \rightarrow J = 1$ transition except that the matrix elements (relative transition probabilities) are kept general. The level diagram is shown in Fig. 1(a). (The notation is slightly different from that in I.) For two opposite circularly polarized fields, Eq. (5) of I can be integrated. After some manipulation we have

$$N_{a1} = N_0 - C_{a1}{}^2(E_-{}^2/E_0{}^2)\gamma_{ab}{}^2[\gamma_{ab}{}^2 + (\omega_{a1} - \nu_- + kv)^2]^{-1}N_{a1} - C_{a1}{}^2(E_+{}^2/E_0{}^2)\tfrac{1}{2}(\gamma_{ab}\gamma_b)[\gamma_{ab}{}^2 + (\omega_{a2} - \nu_+ + kv)^2]^{-1}N_{a2}$$

$$- C_{a1}C_{a2}(E_-E_+/E_0{}^2)\{\tfrac{1}{2}\gamma_{ab}[\rho_{12}'(\gamma_{ab} + i(\omega_{a1} - \nu_- + kv))^{-1} + \rho_{12}'^*(\gamma_{ab} - i(\omega_{a1} - \nu_- + kv))^{-1}]$$

$$+ (\tfrac{1}{4}\gamma_b)[\rho_{12}'(\gamma_{ab} - i(\omega_{a2} - \nu_+ + kv))^{-1} + \rho_{12}'^*(\gamma_{ab} + i(\omega_{a2} - \nu_+ + kv))^{-1}]\}. \quad (1)$$

$N_{a2} =$ same as N_{a1} but with $+$ and $-$ and 1 and 2 subscripts interchanged.

---

[1] A. Dienes, preceding paper, Phys. Rev. **174**, 400 (1968), hereafter referred to as I.